

(19) World Intellectual Property Organization  
International Bureau



(43) International Publication Date  
4 December 2003 (04.12.2003)

PCT

(10) International Publication Number  
WO 03/099536 A1

(51) International Patent Classification<sup>7</sup>: B29C 43/36

(21) International Application Number: PCT/US03/18020

(22) International Filing Date: 27 May 2003 (27.05.2003)

(25) Filing Language: English

(26) Publication Language: English

(30) Priority Data:  
60/382,961 24 May 2002 (24.05.2002) US  
10/244,276 16 September 2002 (16.09.2002) US

(71) Applicants and

(72) Inventors: CHOU, Stephen, Y. [US/US]; 7 Foulet Drive, Princeton, NJ 08540 (US). ZHANG, Wei [CN/US]; 41-07 Ravens Crest Drive, Plainsboro, NJ 08536 (US).

(74) Agent: BOOKS, Glen, E.; Lowenstein Sandler PC, 65 Livingston Avenue, Roseland, NJ 07068 (US).

(81) Designated States (*national*): AE, AG, AL, AM, AT, AU, AZ, BA, BB, BG, BR, BY, BZ, CA, CH, CN, CO, CR, CU, CZ, DE, DK, DM, DZ, EC, EE, ES, FI, GB, GD, GE, GH, GM, HR, HU, ID, IL, IN, IS, JP, KE, KG, KP, KR, KZ, LC, LK, LR, LS, LT, LU, LV, MA, MD, MG, MK, MN, MW, MX, MZ, NI, NO, NZ, OM, PH, PL, PT, RO, RU, SC, SD, SE, SG, SK, SL, TJ, TM, TN, TR, TT, TZ, UA, UG, US, UZ, VC, VN, YU, ZA, ZM, ZW.

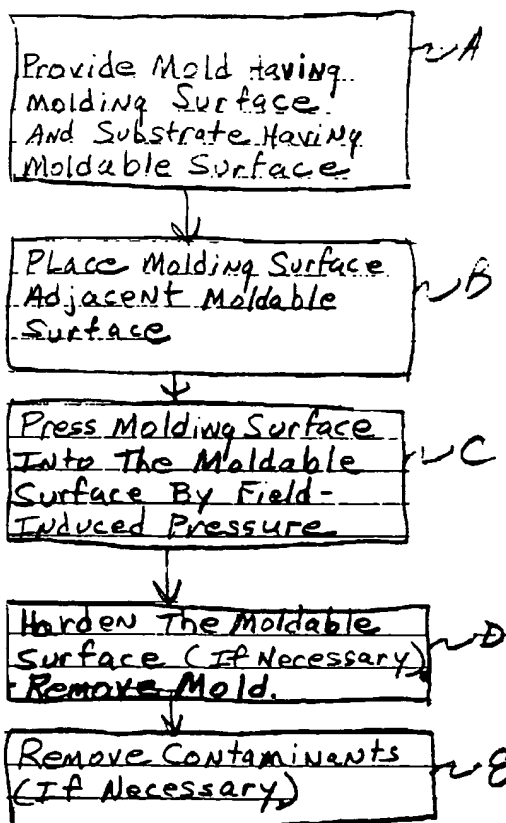
(84) Designated States (*regional*): ARIPO patent (GH, GM, KE, LS, MW, MZ, SD, SL, SZ, TZ, UG, ZM, ZW), Eurasian patent (AM, AZ, BY, KG, KZ, MD, RU, TJ, TM), European patent (AT, BE, BG, CH, CY, CZ, DE, DK, EE, ES, FI, FR, GB, GR, HU, IE, IT, LU, MC, NL, PT, RO, SE, SI, SK, TR), OAPI patent (BF, BJ, CF, CG, CI, CM, GA, GN, GQ, GW, ML, MR, NE, SN, TD, TG).

Published:

— with international search report

For two-letter codes and other abbreviations, refer to the "Guidance Notes on Codes and Abbreviations" appearing at the beginning of each regular issue of the PCT Gazette.

(54) Title: METHODS AND APPARATUS OF FIELD-INDUCED PRESSURE IMPRINT LITHOGRAPHY



(57) Abstract: An improved method of imprint lithography involves using fluid-induced pressure from electric or magnetic fields to press a mold onto a substrate having a moldable surface. In essence, the method comprises the steps of providing a substrate having a moldable surface, providing a mold having a molding surface and pressing the molding surface and the moldable surface together by electric or magnetic fields to imprint the molding surface onto the moldable surface. The molding surface advantageously comprises a plurality of projecting features of nanoscale extent or separation, but the molding surface can also be a smooth planar surface, as for planarization. The improved method can be practiced without mechanical presses and without sealing the region between the mold and the substrate.

**METHODS AND APPARATUS OF FIELD-INDUCED PRESSURE  
IMPRINT LITHOGRAPHY**

**CROSS REFERENCE TO RELATED APPLICATIONS**

This application claims the benefit of United States Provisional Patent Application 60/382,961 filed by Stephen Chou and Wei Zhang on May 24, 2002 and entitled "Field-Induced Pressure Imprint Lithography".

This application is a continuation-in-part of United States Patent Application Serial No. 10/244,276 filed by Stephen Chou on September 16, 2002 and entitled "Lithographic Method For Molding Pattern With Nanoscale Features" which, in turn, is a continuation of U.S. Application 10/046,594 filed by Stephen Chou on October 29, 2001, which claims priority to U.S. Patent Application Serial No. 09/107,006 filed by Stephen Chou on June 30, 1998 (now United States Patent No. 6,309,580 issued October 30, 2001) and which, in turn, claims priority to U.S. Application Serial No. 08/558,809 filed by Stephen Chou on November 15, 1995 (now U.S. Patent No. 5,772,905 issued June 30, 1998). All of the foregoing Related Applications are incorporated herein by reference.

This case is also a continuation-in-part of United States Patent Application Serial No. 10/140,140 filed by Stephen Chou on May 7, 2002 and entitled "Fluid Pressure Imprint Lithography" which is a divisional of United States Patent Application Serial No. 09/618,174 filed by Stephen Chou on July

18, 2000 and entitled "Fluid Pressure Imprint Lithography" (now U.S. Patent No. 6,482,742).

### **FIELD OF THE INVENTION**

This invention relates to imprint lithography and, in particular, to imprint lithography wherein electrical or magnetic fields are used to imprint a molding surface onto a moldable surface. The process is particularly useful to provide nanoimprint lithography of enhanced resolution and uniformity over an increased area.

### **BACKGROUND OF THE INVENTION**

Photolithography is a key process in the fabrication of semiconductor integrated circuits and many optical, magnetic and micromechanical devices. Lithography creates a pattern on a thin film carried on a substrate so that, in subsequent process steps, the pattern can be replicated in the substrate or in another material which is added onto the substrate. Conventional lithography typically involves applying a thin film of resist to a substrate, exposing the resist to a desired pattern of radiation, and developing the exposed film to produce a physical pattern. In this approach, resolution is limited by the wavelength of the radiation, and the equipment becomes increasingly expensive as the feature size becomes smaller.

Imprint lithography, based on a fundamentally different principle, offers high resolution, high throughput, low cost and the potential of large area coverage. In imprint lithography, a mold with microscale or

nanoscale features is pressed into a thin film, deforming the shape of the film according to the features of the mold and forming a relief pattern in the film. After the mold is removed, the thin film can be processed to remove the reduced thickness portions. This removal exposes the underlying substrate for further processing. Details of imprint lithography are described in applicant's United States Patent No. 5,772,905 issued June 30, 1998 and entitled "Nanoimprint Lithography". The '905 patent is incorporated herein by reference.

The usual method of pressing the mold into the thin film involves positioning the mold and the substrate on respective rigid plates of a high precision mechanical press. With such apparatus, the process can generate sub-25 nm features with a high degree of uniformity over areas on the order of 12 in<sup>2</sup>. Larger areas of uniformity would be highly advantageous to increase throughput and for many applications such as displays.

The use of a high precision mechanical press to press a mold into a thin film presents tolerance problems in replicating small patterns over large areas. Presses move on guide shafts through apertures, and the spacings between the shafts and their respective apertures can be large compared to the features to be replicated. Such spacings permit undesirable relative translational and rotational shifts between the substrate and the mold. Moreover, despite the most careful construction, the molds and the substrates used in lithography are not perfectly planar. When these molds and substrates are disposed on the rigid plates of a press, the deviations from planarity over large areas can result in variations in the molding pressure and depth of

imprint. Accordingly, it is desirable to provide a method of imprint lithography which avoids the limitations of mechanical presses.

An alternative method of pressing the mold into the thin film is the technique of fluid pressure imprint lithography described in applicant's United States Patent No. 6,482,742 issued November 19, 2002 and entitled "Fluid Pressure Imprint Lithography". In this method the molding surface is disposed adjacent the film, the molding surface/film interface is sealed and pressurized fluid is used to force the molding surface into the film. Since the pressure is isostatic, translational and rotational shifts are minimal, and smaller features can be imprinted with high uniformity over larger areas than can be imprinted using mechanical presses.

Fluid pressure imprinting has dramatically improved nanoimprint lithography. A further improvement for commercial manufacture would be a method which could provide comparable results without the necessity of sealing the molding surface/film interface.

### **SUMMARY OF THE INVENTION**

An improved method of imprint lithography involves using field-induced pressure from electric or magnetic fields to press a mold into a substrate having a moldable surface. In essence, the method comprises the steps of providing a substrate having a moldable surface, providing a mold having a molding surface and pressing the molding surface and the moldable surface together by electric or magnetic fields to imprint the molding surface onto the moldable surface. The molding surface advantageously comprises a plurality of projecting features of nanoscale extent or separation, but the

molding surface can also be a smooth planar surface, as for planarization. The improved method can be practiced without mechanical presses and without sealing the region between the mold and the substrate.

### **BRIEF DESCRIPTION OF THE DRAWINGS**

The advantages, nature and various additional features of the invention will appear more fully upon consideration of the illustrative embodiments now to be described in detail in connection with the accompanying drawings. In the drawings:

Fig. 1 is a schematic flow diagram of the steps in an improved method of imprint lithography;

Fig. 2 illustrates apparatus for practicing the method of Fig. 1 using an electrical field;

Figs. 3A, 3B and 3C show various substrate constructions for facilitating electrical contact with a substrate conductive layer;

Fig. 4 shows an alternative apparatus for practicing the method of Fig. 1 without direct electrical contact;

Fig. 5 illustrates apparatus for practicing the method of Fig. 1 using a magnetic field;

Fig. 6A and 6B show exemplary multilayer mold constructions useful for the apparatus of Figs. 2, 4 and 5; and

Fig. 7 schematically illustrates how the method of Fig. 1 is compatible with a variety of other processing steps.

It is to be understood that these drawing are for purposes of illustrating the concepts of the invention and are not to scale.

### **DETAILED DESCRIPTION**

Referring to the drawings, Fig. 1 is a schematic flow diagram of an improved process for imprint lithography using field-induced pressure. An initial step shown in Block A, is to provide a mold having a molding surface such as plurality of protruding features and a substrate having a surface of moldable material such as one or more moldable thin films. Protruding features are preferably micrometer scale features and, more advantageously, nanoscale features. The method is highly advantageously where the mold surface has at least two spaced apart protruding features. A moldable material is one which retains or can be hardened to retain the imprint of the protruding features from the mold surface.

The next step, shown in Block B, is to place the mold adjacent the moldable surface. If the moldable surface is a thin film that already includes a previously formed pattern, then the pattern of the mold should be carefully aligned with the previous pattern. This can be done by alignment techniques well known in the art.

The third step (Block C) is to press the mold onto the moldable surface by field-induced pressure. One method for doing this is to dispose the assembly between conductive layers and apply an electrical field between the

layers. Another approach is to dispose the assembly between layers of magnetic material and to apply a magnetic field that will force the layers together. The advantage of field-induced pressure is that the resulting force uniformly pushes the mold onto the moldable surface. Shear or rotational components are *de minimus*. Moreover since the mold and/or substrate are flexible rather than rigid, conformation between the mold and the moldable surface is achieved regardless of unavoidable deviations from planarity. The result is an enhanced level of molding resolution, alignment and uniformity over an increased area of the film.

The next step shown in Block D, is to harden the moldable surface, if necessary, so that it retains the imprint of the mold and then to remove the mold. The process for hardening depends on the material of the moldable surface. Some materials will maintain the imprint with no hardening. Thermoplastic materials can be hardened by preliminarily heating them prior to molding and permitting them to cool after imprint. PMMA, for example, can be suitably softened by heating to 120° C prior to molding and hardened by cooling after imprint. Heat curable materials can be hardened by applying heat during imprint. A heater and/or the use of a heated pressurized fluid can thus effectuate such softening or hardening. Radiation curable materials can be hardened by the application of UV radiation during imprint. Silicon can be softened by UV laser radiation to accept imprinting and hardened by cooling to ambient temperature.

The fifth step shown in Block E is optional in some applications. It is to remove contaminants (if any) and excess material from the recesses of the molded surface. The molded surface will typically have



raised features and recesses. In many lithographic operations it is desirable to eliminate the material from the recesses so that the underlying substrate is exposed for further processing. This can be conveniently accomplished using reactive ion etching.

In some applications, the imprinted structure itself is a part of a device to be built. In other applications the resulting structure is a resist-covered semiconductor substrate with a pattern of recesses extending toward the substrate. Such a structure can be further processed in a variety of ways well-known in the art. For example, the molded film can be used as a mask for the removal of surface layers in exposed regions of the substrate, for doping exposed regions of the substrate or for growing or depositing materials on the exposed regions.

Fig. 2 schematically illustrates a first exemplary apparatus 9 for practicing the method of Fig. 1. The apparatus 9 comprises an assembly of a mold 10 having a molding surface 12 and a substrate 20 having a moldable surface 22. The mold and substrate are disposed with the molding surface 12 adjacent the moldable surface 22. The mold 10 comprises a body having a molding surface 12. Surface 12 can include a plurality of protruding features 13 having a desired shape for imprinting onto the moldable surface 22. The molding surface 12 can be patterned into protruding features 13 of nanoscale dimensions by known techniques such as electron beam lithography. The projecting extent of the protruding features 13 is typically in the range 0.1 nm to 200  $\mu\text{m}$ . Typical separations between protruding features are 200 nanometers or less. Advantageously the mold 10 is a multilayer structure comprising a layer of conductive or chargeable material that is distal to the

interface between the molding surface and the moldable surface. The term layer as used herein is intended broadly to cover a supported layer, a plate or a composite layer.

The substrate 20 is typically a solid substrate and the moldable surface 22 is typically a thin film of polymer, monomer, oligomer or combination thereof that is pliable or can be made pliable to pressure and can retain a pressure-imprinted deformation or pattern. It can be a thermoplastic polymer, such as polycarbonate or polymethyl methacrylate (PMMA), which softens in response to heat. Alternately it can be a monomer liquid, such as a curable silicone, which hardens with curing. Yet further in the alternative, it can be solid silicon which can be liquefied by a UV laser pulse. Polymer thin films are typically applied to the substrate by spraying or spinning. Advantageously the film does not adhere to the mold surface. If necessary, the mold surface can be coated with a release agent to prevent such adherence. Advantageously the substrate is a multilayer structure comprising a layer or plate 23 of conductive or chargeable material that is distal to the molding surface/moldable surface interface.

The pressure between the mold and the substrate can be generated by electrical or magnetic forces between the mold and the substrate. For a pressure generated by an electrical force, an attractive electrical field can be established between the mold and the substrate. Alternatively a repulsive field can be used to drive the mold and the substrate together. For a pressure generated by a magnetic force, an attractive magnetic force between the mold and the substrate can provide attractive pressure or repulsive external magnetic forces can drive the mold and the substrate together.

In use, a field forces the molding surface onto the moldable surface. In the embodiment of Fig. 2 where the field is an electric field, this imprinting can be effected by connecting layers 14 and 23 to opposite polarity terminals of a voltage source 30. The voltage from source 30 can be AC, DC, pulsed, or a combination of such voltages.

Electrical connection with layers 14 and 23 can be facilitated by choosing substrate 20 to be conductive and mold 10 to be conductive. Alternatively, conductive through holes (not shown) through substrate 20 to layer 23 and through mold 10 to layer 14 can provide connection. Figs. 3A, 3B and 3C show substrate constructions that facilitate electrical connection with substrate conductive layer 23. In Fig. 3A, electrical contact can be made from the bottom of substrate 20 through conductive vias 30. In Fig. 3B electrical contact can be made from the bottom or from the lateral edges by coating or plating a peripheral layer 31 of conductive material around a portion of the lateral periphery of the substrate 20. A similar peripheral conductive layer 32 is shown in Fig. 3C except that layer 32 does not extend to the bottom of the substrate. Yet further in the alternative, an electric field for imprinting the substrate can be created between appropriately dissimilar materials by the use of light, heat or RF radiation.

In some applications it may be advantageous to make the mold 10 or the substrate 20 (including the conductive layers) of materials at least partially transparent to radiation which can be used to soften or cure the moldable surface.

In other applications it may be desired to omit one of the conductive layers 14, 23 and to use an attractive or repulsive field between an external electrode and the remaining layer to force the molding surface and the moldable surface together.

Fig. 4 shows an alternative apparatus for using an electrical field to press the molding surface into the moldable surface. The apparatus of Fig. 4 is similar to that of Fig. 2 except that rather than directly connecting the layers 14 and 23 to a voltage source, the mold 10/substrate 20 assembly is disposed between electrodes 40 and 41 that are connected to an AC voltage source 42. The frequency of the AC source can be tuned to generate a desired induced voltage between layers 14 and 23.

Fig. 5 illustrates alternative apparatus for practicing the method of Fig. 1. The Fig. 5 apparatus is similar to the apparatus of Fig. 2 except that instead of conductive layers, magnetic layers 14A, 23A are disposed distal to the mold/substrate interface and a magnetic field is used to imprint the mold surface into the moldable surface. The magnetic layers can be magnetizable material, permanent magnets or electromagnets. For example, layers 14A, 23A can comprise helically or spirally wound coils. Current from current sources 50A, 50B applied to coils can produce an attractive magnetic field to press the molding surface onto the moldable surface. Connections between the current sources and their respective coils can be facilitated by conduction through conductive vias (not shown) in the substrate and the mold. In a modified form, layers 14A and 23A can be magnetic materials that attract one another, and the current sources can be omitted. In another variation, the mold can comprise an electromagnet and the substrate can comprise a layer of

magnetizable or permanent magnetic material or vice versa. In essence, what is needed is a magnetic layer and a magnetic field generator interacting with the magnetic layer to press the molding surface and the moldable surface together.

Figs. 6A and 6B show different multilayer mold constructions useful in the embodiments of Figs. 2-5. In Fig. 6A, the conductive or magnetic layer 14 is disposed immediately distal to the interface between the molding surface 12 and the moldable surface (not shown). In Fig. 6B, the conductive or magnetic layer 14 is still distal to the interface on the mold side, but there is an intervening layer 60.

It is further contemplated that field-induced imprinting can be used in conjunction with other methods of providing imprint pressure such as direct fluid pressure or mechanical pressure in all possible permutations in applying these forces, including applying them simultaneously, sequentially, or selectively.

Fig. 7 schematically illustrates additional steps compatible with the process described herein. Precision mechanical pressing or pressurized fluid pressing can be of supplemental use, particularly after the molding surface is engaged with the moldable layer. Radiation, such as infrared or ultraviolet, can be used for heating, softening, or curing the moldable surface material. The layers 14, 23 can be conductive or magnetic, and the pressing fields can be DC, AC, or combinations thereof.

It is to be understood that the above described embodiments are illustrative of only a few of the many embodiments which can represent

applications of the invention. Numerous and varied other arrangements can be made by those skilled in the art without departing from the spirit and scope of the invention.

**WHAT IS CLAIMED:**

1. A method for processing a moldable surface comprising the steps of:

providing a substrate having the moldable surface;

providing a mold having a molding surface;

pressing the molding surface and the moldable surface together by electric or magnetic field-induced pressure to imprint the molding surface onto the moldable surface; and

withdrawing the mold from the moldable surface.

2. The method of claim 1 wherein the moldable surface comprises one or more moldable layers disposed on the substrate.

3. The method of claim 2 wherein the imprinting produces reduced thickness regions in the moldable layer and further comprising the steps of:

removing the material of the moldable layer from the reduced thickness regions to selectively expose regions of the substrate; and

further processing the substrate selectively in the exposed regions.

4. The method of claim 3 wherein the further processing comprises doping the substrate with impurities, removing material from the substrate, or adding material on the substrate.

5. The method of claim 1 further comprising the step of hardening the moldable surface after pressing.

6. The method of claim 1 wherein the substrate or the mold or both are sufficiently flexible to conform together under the pressure.

7. The method of claim 2 where the thickness of the moldable layer is in the range 0.1 nm to 200  $\mu\text{m}$ .

8. Apparatus for imprinting a moldable surface on a substrate comprising:

a mold having a molding surface;

a substrate having a moldable surface positioned adjacent the molding surface of the mold;



a first chargeable or conductive layer disposed distal to the moldable surface/molding surface interface on the mold side of the interface;

a second chargeable or conductive layer disposed distal to the moldable surface/molding surface interface on the moldable surface side of the interface; and

means for forming an electrical field between the first and second layers to press the molding surface and the moldable surface together.

9. The apparatus of claim 8 wherein at least one of the first and second layers is conductive and the means for forming an electrical field comprises a voltage source.

10. The apparatus of claim 9 wherein the first and second layers comprise conductive material.

11. The apparatus of claim 9 wherein the voltage source comprises a DC voltage source.

12. The apparatus of claim 9 wherein the voltage source comprises an AC voltage source.

13. The apparatus of claim 9 wherein the voltage source comprises a pulsed voltage source.

14. The apparatus of claim 9 wherein the voltage source can provide a combination of DC, AC and pulsed voltage.

15. The apparatus of claim 9 wherein the mold includes a conductive layer.

16. The apparatus of claim 10 wherein the voltage source is connected between the layers of conductive material.

17. The apparatus of claim 9 wherein the mold and the substrate are disposed between at least two external electrodes and the means for forming an electrical field comprises a voltage source to apply a voltage between the external electrodes.

18. The apparatus of claim 17 wherein the voltage source is an AC or pulsed voltage source.

19. Apparatus for imprinting a moldable surface on a substrate comprising:

a mold having a molding surface;

a substrate having a moldable surface positioned adjacent the molding surface;

a magnetic layer disposed distal to the moldable surface/molding surface interface;

and a magnetic field generator to generate a magnetic field interacting with the first magnetic layer to press the molding surface and the moldable surface together.

20. The apparatus of claim 19 wherein the magnetic layer comprises a conductive coil or spiral.

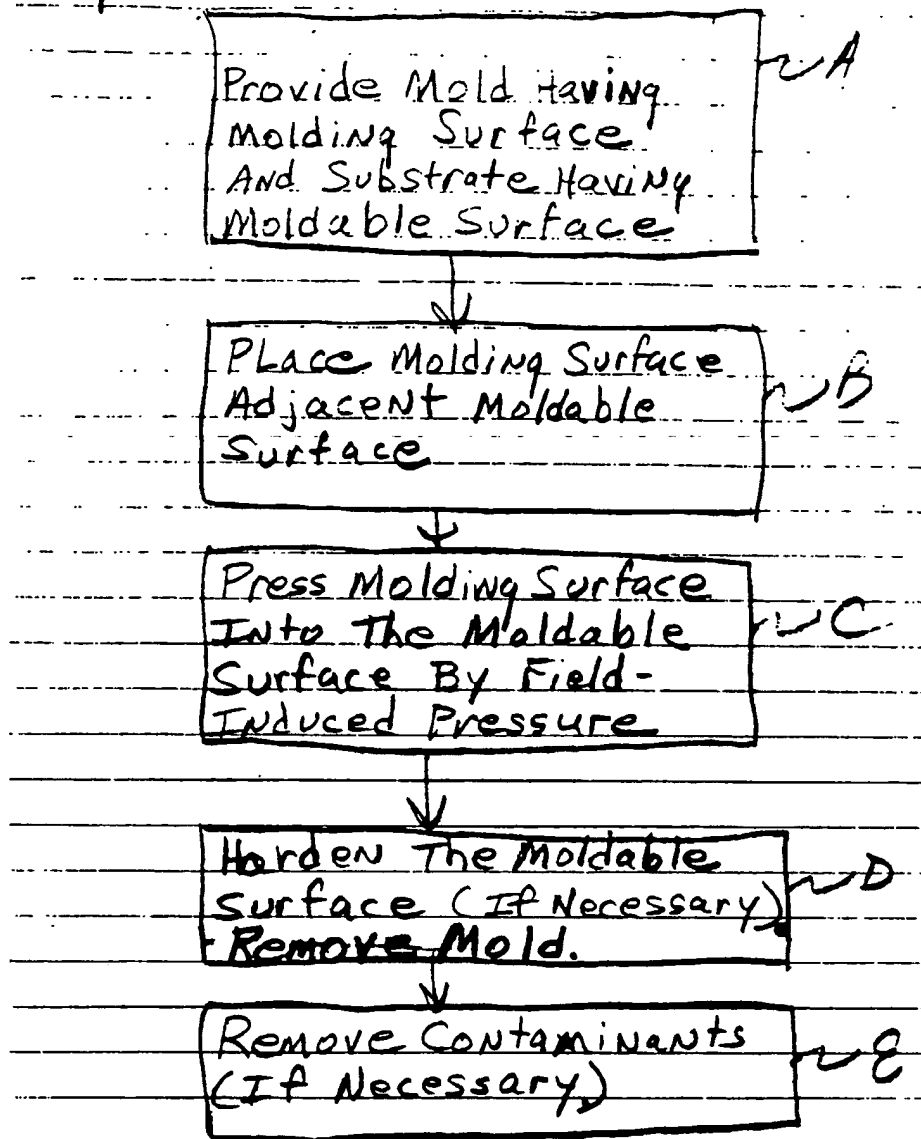
21. The apparatus of claim 19 wherein the magnetic field generator comprises a conductive coil or spiral.

22. The apparatus of claim 19 wherein the magnetic layer comprises a layer of magnetized material.

23. The apparatus of claim 19 wherein the magnetic layer comprises a layer of magnetizable material.

24. The method of claim 1 further comprising the step of applying imprint pressure mechanically or as direct fluid pressure.

Fig. 1



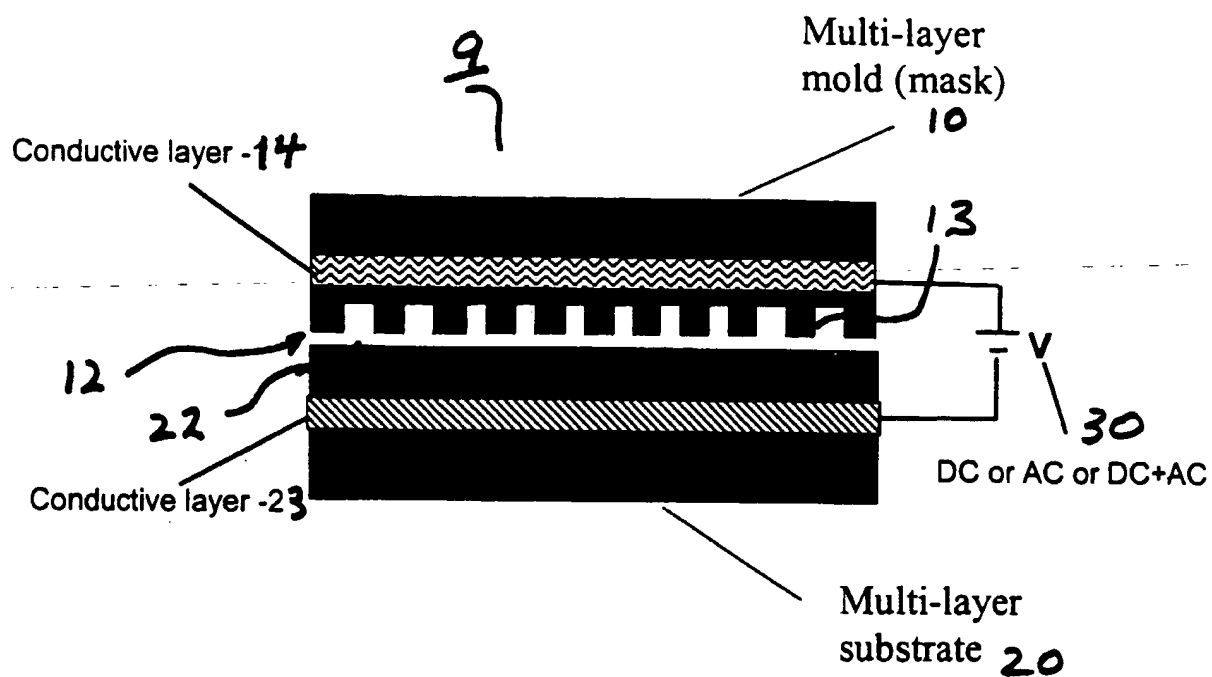
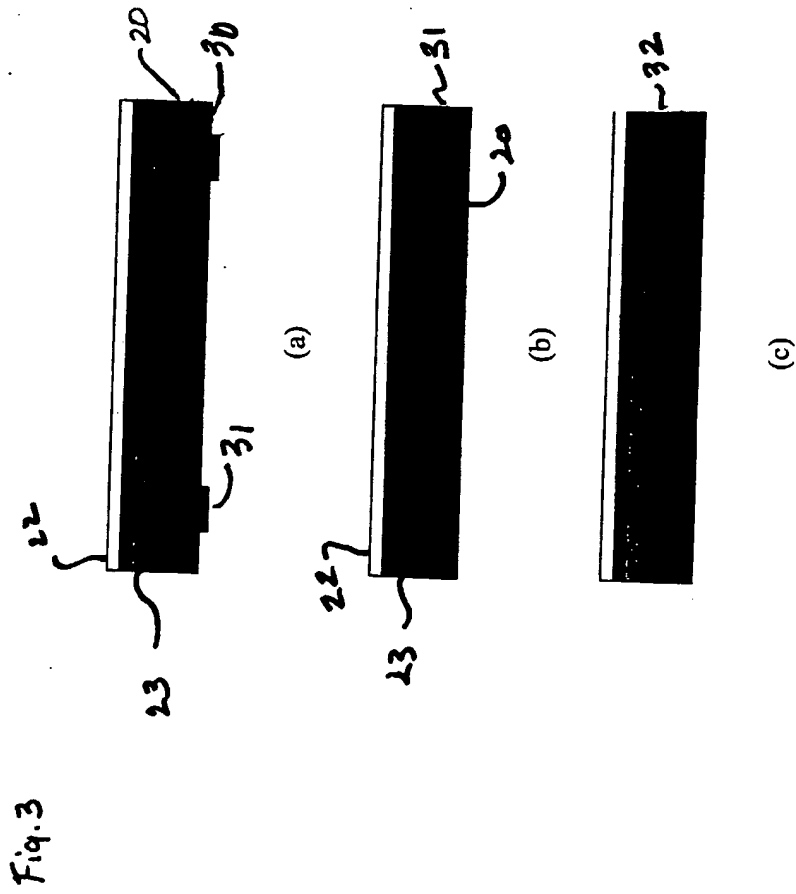


Fig. 2



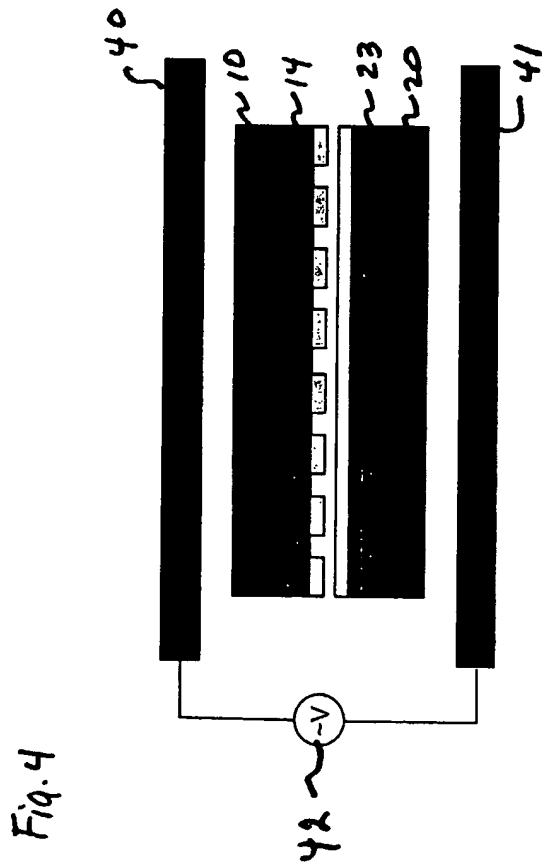




Fig. 5

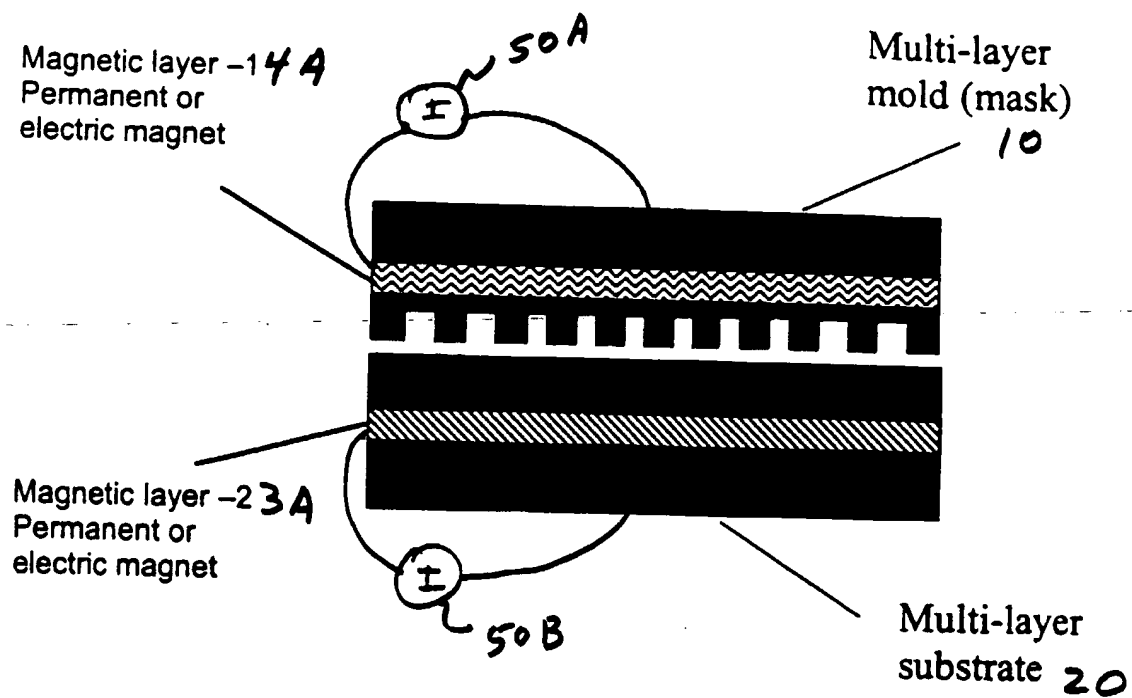
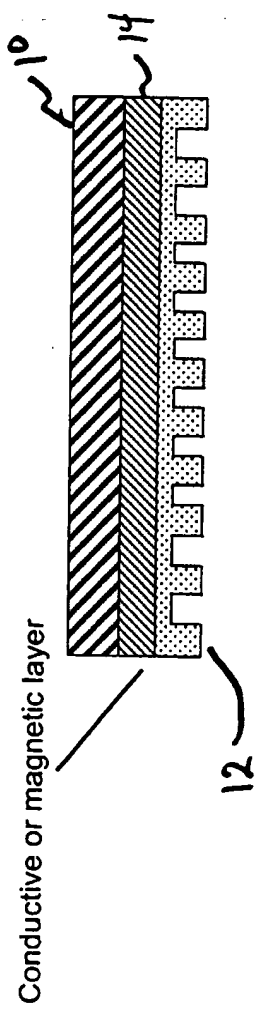
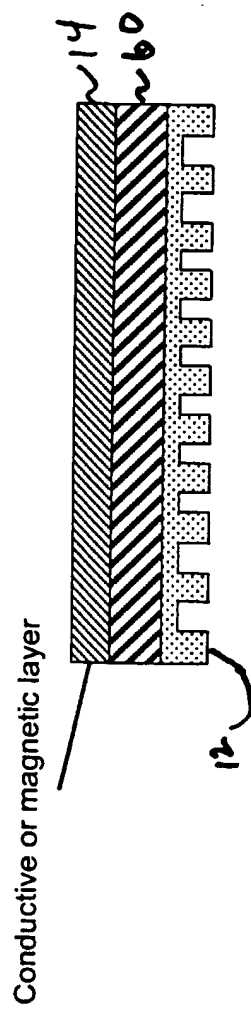


Fig. 6

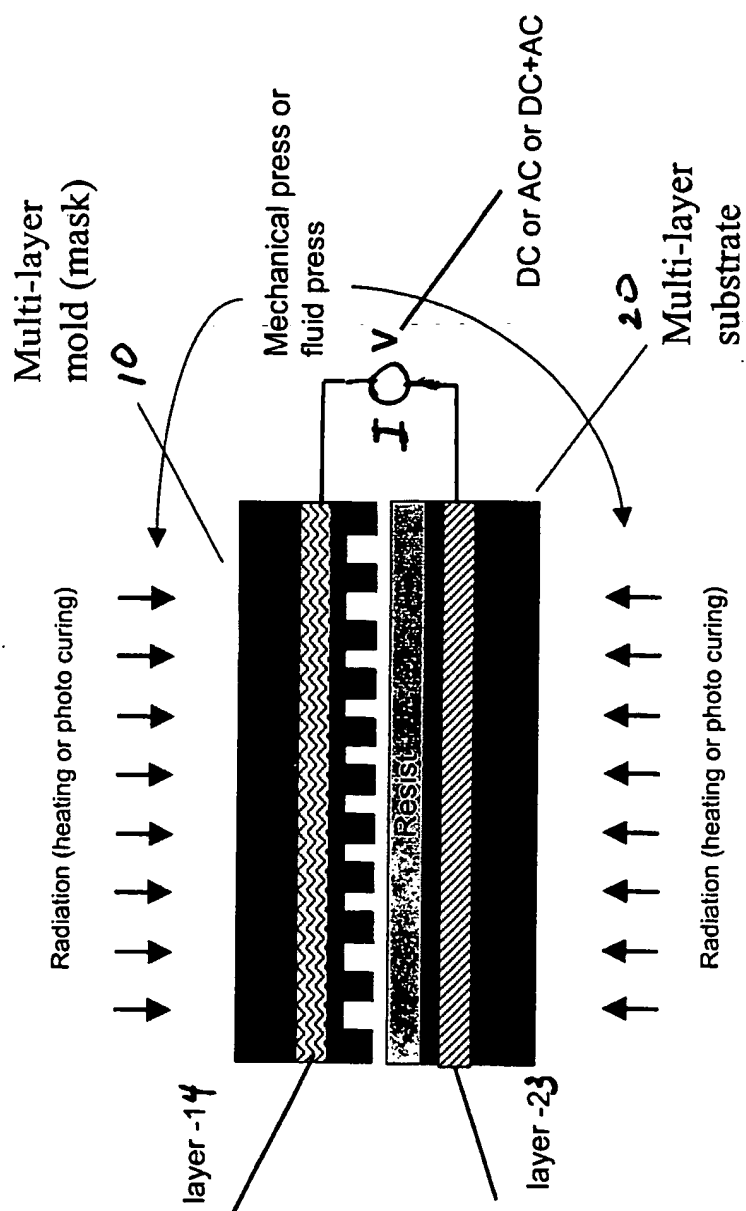


(a)



(b)

Fig. 7



# Characterization and modeling of volumetric and mechanical properties for step and flash imprint lithography photopolymers

Matthew Colburn, Itai Suez, Byung Jin Choi, Mario Meissl, Todd Bailey, S. V. Sreenivasan, John G. Ekerdt, and C. Grant Willson<sup>a)</sup>

*Texas Materials Institute, The University of Texas at Austin, Austin, Texas 78712*

(Received 1 June 2001; accepted 1 October 2001)

Step and flash imprint lithography (SFIL) is an alternative approach to high-resolution patterning based on a bilayer imprint scheme. SFIL utilizes the *in situ* photopolymerization of an oxygen etch resistant monomer solution in the topography of a template to replicate the template pattern on a substrate. The SFIL replication process can be affected significantly by the densification associated with polymerization and by the mechanical properties of the cured film. The densities of cured photopolymers were determined as a function of pendant group volume. The elastic moduli of several photopolymer samples were calculated based on a Hertzian fit to force–distance data generated by atomic force microscopy. The current SFIL photopolymer formulation undergoes a 9.3% (v/v) densification. The elastic modulus of the SFIL photopolymer is 4 MPa. The densification and the elastic modulus of the photopolymer layer can be tailored from 4% to 16%, and from 2 to 30 MPa, respectively, by changing the structure of the photopolymer precursors and their formulation. The complex interaction among densification, mechanical properties (elastic modulus and Poisson's ratio) and aspect ratio (height:width) was studied by finite element modeling. The effect of these parameters on linewidth, sidewall angle, and image placement was modeled. The results indicate that the majority of densification occurs by shrinkage in the direction normal to the substrate surface and that Poisson's ratio plays a critical role in defining the shape of the replicated features. Over the range of material properties that were determined experimentally, volumetric contraction of the photopolymer is not predicted to adversely affect either pattern placement or sidewall angle. © 2001 American Vacuum Society. [DOI: 10.1116/1.1420199]

## I. INTRODUCTION

Step and flash imprint lithography (SFIL) is a patterning process utilizing photopolymerization to replicate the topography of a template onto a substrate.<sup>1,2</sup> Polymerization, however, is often accompanied by densification. The interaction potential between photopolymer precursors undergoing free radical polymerization changes from Van der Waals' to covalent. The average distance between the molecules decreases and causes volumetric contraction. Densification of the SFIL photopolymer (the etch barrier) may affect both the cross sectional shape of features and the placement of relief patterns. Finite element modeling (FEM) makes it possible to explore the influence of densification and mechanical properties on changes in the placement and in the geometry of the replicated features. The densification and elastic modulus of prospective etch barrier candidates have been characterized and were used as the basis for the physical properties in FEM simulation.

## II. EXPERIMENTAL METHODS

The densities of the photopolymers were determined by Archimedes' principle. In these experiments, dry samples  $T_1$  were first weighed in air. Then the samples  $T_2$  were weighed while submerged in a fluid of known density  $\rho_{\text{liq}}$ . Equation

(1) relates the density of the sample  $\rho_{\text{sample}}$  to the difference in the measured weights. The volumetric change was calculated using Eq. (2):

$$\rho_{\text{sample}} = \rho_{\text{liq}} \left( \frac{T_1}{T_2} \right), \quad (1)$$

$$\Delta V = \left( \frac{\rho_{\text{polymer}} - \rho_{\text{monomer}}}{\rho_{\text{polymer}}} \right). \quad (2)$$

The elastic modulus of the etch barrier films was characterized by nanoindentation on a Thermomicroscope CP Research atomic force microscope (AFM) equipped with an Ultralever B tip which has a spring constant of 0.4 N/m. The calibration procedure prescribed by Thermomicroscopes for the force–distance analysis was performed on each Ultralever B tip.<sup>3</sup> In the nanoindentation process, the AFM cantilever is actuated toward the sample a distance  $z$ . When the tip comes in contact with the sample, the cantilever is deflected a distance  $d$ . The force imparted on the sample is directly proportional to this deflection by the spring constant  $k$  of the cantilever. This force results in the indentation of the sample to a depth  $\delta$ . The cantilever travel is equal to the deflection plus the indentation depth ( $z = d + \delta$ ).

The contact mechanics of a tip impinging on a surface have been extensively studied.<sup>4–6</sup> Several models were considered, but the Hertzian model has proved to be more robust for these samples and was used to analyze all force–distance data.<sup>4</sup> In the Hertzian model, the material is assumed to be

<sup>a)</sup> Author to whom correspondence should be addressed; electronic mail: willson@che.utexas.edu

have isotropically and have no attractive forces that distort the contact area between the tip and the substrate, and the indenter is assumed to have a spherical tip of radius  $R$ . Under these assumptions, the observed force  $F$  obeys the following equation:

$$F = (K^2 R \delta^3)^{1/2}, \quad (3)$$

where

$$\frac{1}{K} = \frac{3}{4} \left( \frac{1 - \nu_s^2}{E_s} + \frac{1 - \nu_{\text{tip}}^2}{E_{\text{tip}}} \right),$$

$\nu$  is Poisson's ratio and  $E$  is the tensile modulus. Since the modulus of the AFM tip  $E_{\text{tip}}$  is much greater than the modulus of the samples  $E_s$ , the second part of the quotient is approximately zero. Linear regression of the force against  $\delta^{3/2}$  yields a slope that is equal to  $4E_s/(3(1 - \nu_s^2))$ . The elastic modulus can be calculated if Poisson's ratio is known. We have approximated this value at 0.35.

Solid models of the etch barrier layer in SFIL were developed using Pro/E®, a commercially available computer aided design package, and analyzed using FEM techniques in Pro/E Mechanical®. The isotropic densification of the etch barrier was simulated using pseudocoefficients of thermal expansion (CTE) defined as the volumetric shrinkage of the etch barrier divided by 1 °C. A model was created at a reference temperature and assigned physical properties ( $E$ ,  $\nu$ , CTE). Rigid interfaces were modeled as fixed boundaries. The temperature of the model was modulated by 1 °C, which resulted in the defined isotropic volumetric contraction. The final state of each model was then compared to the model in the reference state. These models actually simulate a worst-case scenario in which the photopolymerization is completed isotropically in the reference state, then allowed to contract to the model state. Two sets of simulations were performed to identify the effect that pattern layout might have on pattern placement and the effects that etch barrier properties have on feature shape.

The pattern placement study was performed on the pattern shown in the top down view in Fig. 1(a). In the reference state, the features are 200 nm tall. The lines and boxes are separated by 100 nm. The boxes are 2  $\mu\text{m}$  by 2  $\mu\text{m}$  squares. The length of the central line that runs along the boxes is 7.6  $\mu\text{m}$  long. The line that is perpendicular to the central line is 2.5  $\mu\text{m}$  long. The base layer is 100 nm thick and the rigid boundary condition fixed at the bottom of the base layer. The top of the etch barrier was free. The modulus of the etch barrier was 1.6 MPa and Poisson's ratio was estimated at 0.3. The etch barrier densification is 10% (v/v). The motion of the 7.6  $\mu\text{m}$  long centerline was analyzed at the base of the features for displacement motion in-plane with the substrate. This in-plane displacement magnitude was defined as shown below:

$$D_{\text{in-plane}} = \sqrt{\delta_x^2 + \delta_y^2}, \quad (4)$$

where  $\delta_x$  and  $\delta_y$  are orthogonal displacement vectors that are parallel to the substrate surface.

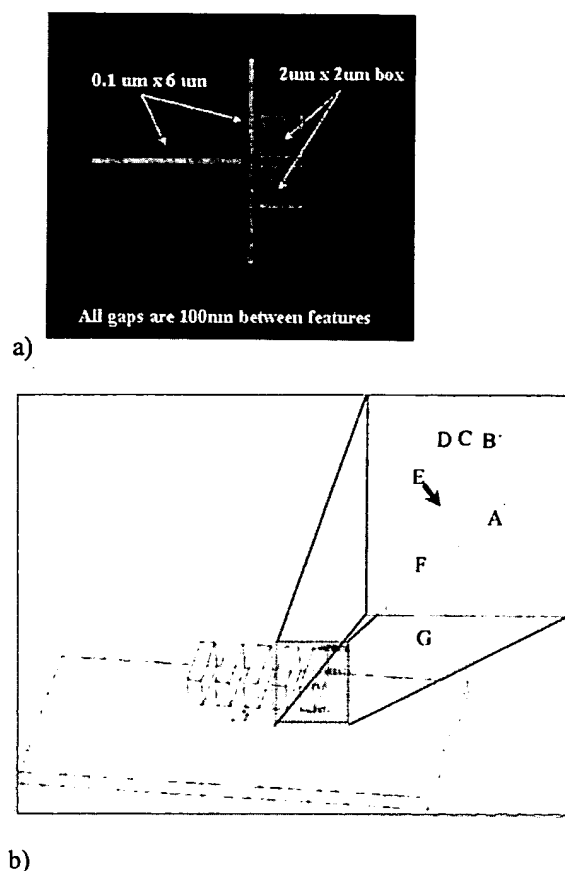


FIG. 1. (a) Pattern placement model. (b) Model used for the full factorial simulations.

The second set of simulations modeled the effect of the aspect ratio, Poisson's ratio, and elastic modulus on the geometry of dense features. The model system is shown in Fig. 1(b). A rigid bottom surface of base layer was used to simulate a transfer layer with a modulus much greater than that of the etch barrier. The reference points are labeled A–G. The displacements of these points were used to calculate the change in length, height, and sidewall. The sidewall angles were determined by the dot product of the vectors defined by the lines  $AE$  and  $AB$ , and lines  $AE$  and  $DE$ . A symmetric boundary condition was placed through the center of the model, halfway along the length of the features. The simulations were performed using a full factorial design of experiment on the 200 nm tall feature with linewidths of 100 nm, 500 nm, 1  $\mu\text{m}$ , and 10  $\mu\text{m}$ , and densifications of 3%, 6.0%, 11.5%, and 17%. The features had a length to width ratio of 10 and a 1:1 pitch (linewidth: line space) except for the 10  $\mu\text{m}$  features which had a length to width ratio of 1:1. The base layer was 100 nm. The elastic modulus and Poisson's ratio were 1 MPa and 0.5, respectively.

In addition to the above simulations, Poisson's ratios of 0.3 and 0.4 were applied to models with densification of 6.0% and 11.5% and linewidths of 100 nm, 500 nm, and 1  $\mu\text{m}$ . Also, 200 nm wide lines having a Poisson's ratio of 0.5 were simulated for densifications of 3% and 17%.

### III. RESULTS

The effect of pendant group size on densification was investigated for a series of monomers that undergo free radical polymerization. Ethyl acrylate, butyl acrylate, hexyl acrylate, lauryl acrylate, 2-(acryloxyethoxy)trimethylsilane (SIA 0160, Gelest), (3-acryloxypropyl) dimethylmethoxysilane (SIA 0190, Gelest), (3-acryloxypropyl) methylbis(trimethylsiloxy)silane (SIA 0194, Gelest), ((3-acryloxypropyl)-tris(trimethylsiloxy)silane (SIA 0210, Gelest), acryloxytrimethylsilane (SIA 0320, Gelest), methacryloxyethoxytrimethylsilane (SIM 6481, Gelest), methacryloxypropyltris(trimethylsiloxy)silane (SIM 6487.6, Gelest), and ~900 molecular weight monomethacryloxypropyl terminated polydimethylsiloxane (MCR-M11, Gelest) monomer solutions were formulated with 1 mole % of 1,3-bis(3-methacryloxypropyl) tetramethyldisiloxane (SIB 1402.0, Gelest) and 1.6 mole % of 1:1 (w/w) mixture of bis(2,4,6-trimethylbenzoyl)-phenylphosphineoxide (Irgacure 819, Ciba) and 1-benzoyl-1-hydroxycyclohexane (Irgacure 184, Ciba); then cured under an  $N_2$  purge. The incorporation of SIB 1402.0, a crosslinker, produces a solid sample that is easily handled.

HyperChem<sup>®</sup> molecular dynamic simulations were utilized to determine the molecular volume ( $\text{\AA}^3$ ) of four alkyl acrylates and the eight silylated monomers. The volumes of acrylic acid and methacrylic acid were simulated and their volumes were defined as the reactive volumes for the acrylic and methacrylic monomers, respectively. The pendant group volume for each monomer was defined as the volume of the monomer minus the reactive volume. A plot of the densification against the volume fraction of the pendant group is shown in Fig. 2(a). The densification of alkyl acrylate monomers ( ) starts at 16.5% for ethyl acrylate and decreases with increasing pendant group volume to a value of 6% for lauryl acrylate. The densification of the silylated monomers ( ) follows a trend similar to that of the organic monomers [Fig. 2(a)]. The pendant group volume effectively dilutes the effect of the densification caused by the generation of covalent bonds formed during photopolymerization of the acrylate.

Since the etch barrier is a blend of two principle components: butyl acrylate and SIA0210, it is necessary to study the effect that blending monomers has on the volumetric change. Butyl acrylate and SIA 0210 were mixed at 25% (w/w) intervals from 100% butyl acrylate to 100% SIA0210. 1% (w/w) SIB1402 and 3% (w/w) of the 1:1 mixture of Irgacure 819 and Irgacure 184 were added to these solutions. The resulting mixtures were cured, their densities measured, and their volume change calculated [Fig. 2(b)]. The system behaves ideally; there is no interaction present in this system. The densification of the current etch barrier formulation is 9.3% (v/v). It consists of 50% (w/w) *n*-butyl acrylate, 50% (w/w) SIA 0210, to which 5% (w/w) SIB 1402, and 3% (w/w) of 1:1 mixture of Irgacure 819 and Irgacure 184 were added.

The elastic moduli of prospective etch barrier components were evaluated by Hertzian fits to data gathered during the nanoindentation experiments. The modulus of SIM 6481 and

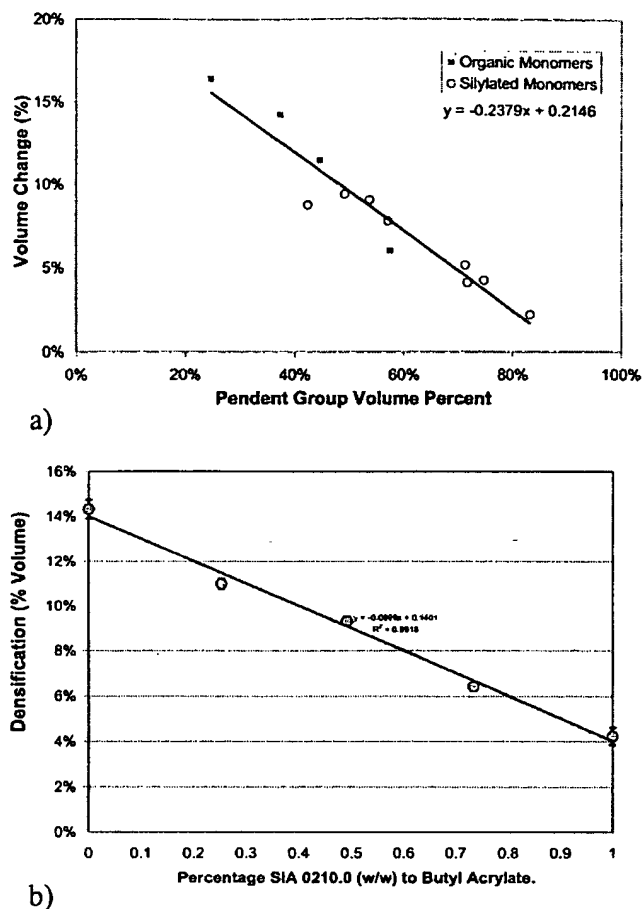


FIG. 2. (a) Volumetric contraction as a function of molecular volume ( $\text{\AA}^3$ ). (b) Densification of 3-acryloxypropyl tris(trimethylsiloxy)silane and butyl acrylate blends.

methacryloxypropylpentamethyl disiloxane (SIM 6487, Gelest) were calculated to be 18.5 and 30 MPa, respectively. The moduli of ethyl acrylate, butyl acrylate, and hexyl acrylate were all calculated to be 2 MPa. The range of elastic moduli could be further extended higher by incorporation of high glass transition monomers, such as methyl methacrylate, norbornene, or styrene, which are capable of free radical polymerization.

Blends of SIA 0210 and butyl acrylate, containing 3% (w/w) of a 1:1 mixture of Irgacure 819 and Irgacure 184 and 1% (w/w) SIB 1402, were cured with ultraviolet light under either a quartz template or a poly(ethylene) sheet to obtain thin crosslinked films on the order of 1–10  $\mu\text{m}$  thick. Figure 3 shows the moduli calculated from force versus distance data for the set of SIA 0210-butyl acrylate blends. The modulus of the film increases linearly with the percent of SIA 0210. The modulus of the SIA 0210, the etch barrier, and *n*-butyl acrylate were calculated at 7.7, 4.2, and 2.1 MPa, respectively.

The pattern simulation was performed to determine whether catastrophic errors in pattern placement would result from the densification of the etch barrier. The reference model incorporated an elastic modulus of 1.6 MPa, a 10% (v/v) densification, and a Poisson's ratio of 0.3. A horizontal

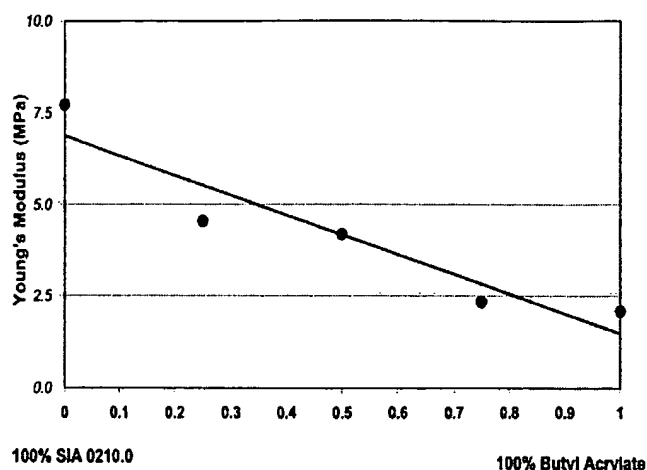


FIG. 3. Elastic moduli of butyl acrylate—3-acryoxypropyl tris(trimethylsiloxy)silane solutions.

cross section of the “in-plane” displacement magnitude was taken just above the feature base. The color-coded image of the in-plane pattern motion is shown in Fig. 4. The key point of interest is the movement of the line as it runs across the  $2\ \mu\text{m} \times 2\ \mu\text{m}$  blocks in the pattern. The “in-plane” displacement of the line was found to be less than 1 nm. A simulation using another FEM package, COSMOS<sup>®</sup>, corroborated this result. Both simulations predict that there will be no local pattern density effect in the SFIL resulting from volumetric contraction of the etch barrier.

A set of simulations was performed on 500 nm wide features, 200 nm tall features on a 100 nm base layer with a Poisson's ratio of 0.5. The modulus ranged from 1 MPa to 1 GPa. The simulations revealed that the tensile modulus of the photopolymerized material does not affect feature shape. Densification fixes the strain at the etch barrier-transfer layer interface; Poisson's ratio dictates how the stress is translated in the direction normal to the applied strain. While the modulus may affect the separation process, it does not affect the feature profiles.

The influence of densification and Poisson's ratio on the cross section of features with width ranging from 100 nm to  $10\ \mu\text{m}$  has been investigated. For the simulations, the verti-

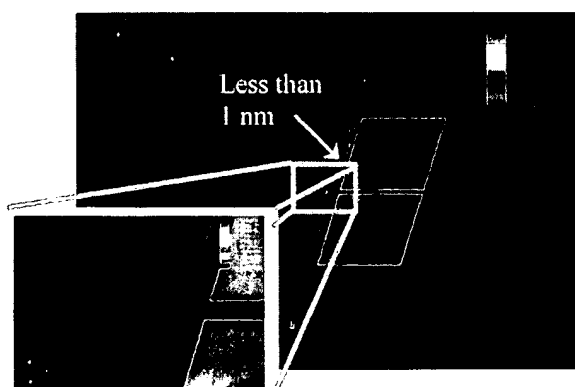
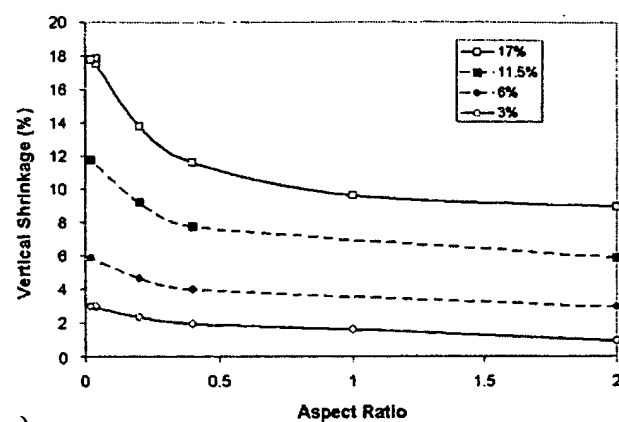
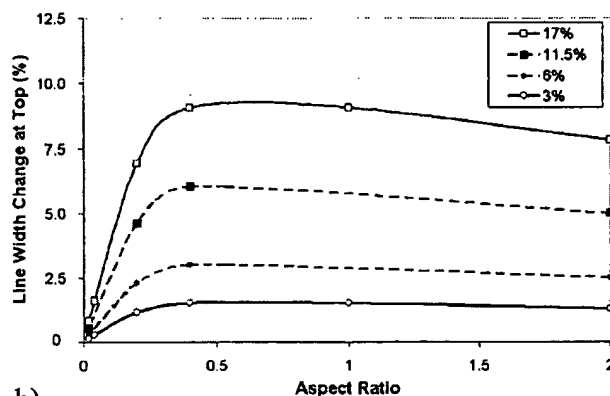


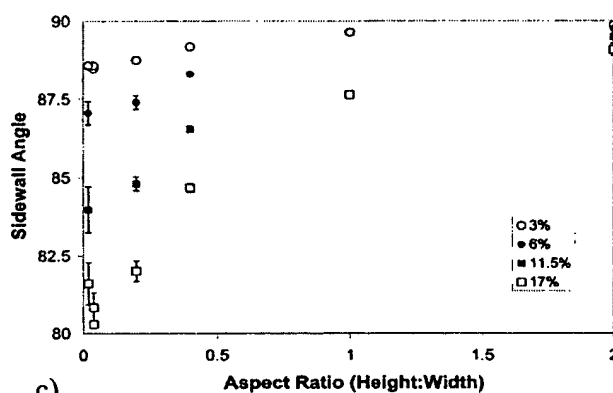
FIG. 4. In-plane motion of pattern (units are in microns).



a)



b)



c)

FIG. 5. (a) Vertical shrinkage of etch barrier features. (b) Effect of densification and Poisson's ratio on linewidth shrinkage. (c) Effect of densification and Poisson's ratio on sidewall angle.

cal shrinkage was measured from the center of the feature [point C in Fig. 1(b)] in a dense spacing. This height was subtracted from the average height of the feature base taken on the left [point E in Fig. 1(b)] and right side [point A in Fig. 1(b)]. The ratio of this height to the original height, 200 nm, is reported in Fig. 5(a). The densification of the monomer and the Poisson's ratio both affect the vertical shrinkage significantly. The maximum vertical shrinkage predicted by the simulation is  $\sim 17\%$  for a Poisson's ratio of 0.5 and 17% densification. This maximum occurs in the center of the feature that experiences the greatest vertical shrinkage. This

point represents the worst-case scenario for the replication process.

The linewidth was measured at the top of the feature after densification and compared to the original width. The change in linewidth predicted by the simulation is shown in Fig. 5(b). The plot indicates that densification plays a major role in linewidth shrinkage. The percent change decreases as the features get wider but the absolute amount of linewidth change increases. In the worst case of 17% (v/v) densification, the actual distance at the top of the features that the linewidth changes approaches a limiting value of 80 nm for 200 nm tall features. The percent change in linewidth at the top of the feature associated with the densification is small; the worst case being 9.1% (or 20 nm of a 200 nm wide feature) for 17% densification and 0.5 Poisson's ratio. It should be noted that the linewidth change at the base of the features was computed and was less than 2.3% for even the worst case. For materials similar to the etch barrier (1 MPa, 8.9% densification,  $\nu=0.4$ ), the linewidth change at the base of the feature was less than 0.3%.

The convolution of linewidth change and vertical shrinkage manifests itself in sidewall angle changes. Analysis of the resulting sidewall angle revealed a linear relationship with aspect ratio. Figure 5(c) shows that the sidewall angle is closer to 90° for smaller features than for larger features. The sidewall angle approaches 80° for small aspect ratio features with 17% densification and Poisson's ratio of 0.5. The line end angle was also studied as a function of aspect ratio; it follows a trend similar to that of sidewall to aspect ratio. As the aspect ratio becomes small, the difference between the sidewall angle and line end angle becomes very small.

## IV. CONCLUSIONS

Photopolymerization of the acrylate systems used in SFIL are accompanied by volumetric contraction. This photopolymerization-induced densification is structure de-

pendent and can be tailored from 2% to 14%. The moduli of several prospective etch barrier monomers were obtained from Hertzian fits to AFM force-distance data. The modulus of the etch barrier formulation is tunable over a range of 2–30 MPa with the current acrylate functionality.

FEM analysis predicts that pattern placement will not be a problem for the current etch barrier formulation. It also predicts that densification will manifest itself mainly in the direction normal to the substrate surface. Linewidth change is a small percentage of the original linewidth. Sidewall angle and line end angle are aspect ratio and material property dependent. The effect of densification will be most prominent in isolated trenches. The sidewall angle for the 10  $\mu\text{m}$  feature is greater than 80° for densification less than 17% and greater than 85° for densification less than 6.0%. These are reasonable profiles to etch transfer into the transfer layer with minimal bias associated with the subsequent reactive ion etch. We are now engaged in experiments designed to test these predictions.

## ACKNOWLEDGMENTS

The authors appreciate the continued support of DARPA (Contract No. MDA972-97-1-0010) and SRC (Contract No. 96-LC-460). They extend special thanks to Larry Fire from PTC for the donation of Pro/E and Pro/Mechanica. They would also like to thank Cindy Stowell, Lindsay Pell, and Professor Brian Korgel (UT-Austin) for their time and for the use of the AFM.

<sup>1</sup>M. Colburn *et al.*, Proc. SPIE 3676, 379 (1999).

<sup>2</sup>M. Colburn, A. Grot, M. Amistoso, B. J. Choi, T. Bailey, J. G. Ekerdt, S. V. Sreenivasan, J. Hollenhorst, and C. G. Willson, Proc. SPIE 3676, 379 (2000).

<sup>3</sup>*User's Guide to AutoProbe CP* (Park Scientific Instruments, Sunnyvale, CA, 1998).

<sup>4</sup>H. J. Hertz, *J. Reine Angew Math.* 92, 156 (1882).

<sup>5</sup>I. N. Sneddon, *Int. J. Eng. Sci.* 2, 47 (1965).

<sup>6</sup>K. L. Johnson, *Contact Mechanics* (Cambridge University Press, Cambridge, 1987).